JOURNAL OF GEOPHYSICAL RESEARCH, VOL. 113, D05204, doi:10.1029/2007JD008962, 2008

Satellite-based estimate of the direct and indirect aerosol climate forcing

Johannes Quaas,[1] Olivier Boucher,[2] Nicolas Bellouin,[2] and Stefan Kinne[1]

Received 14 May 2007; revised 31 October 2007; accepted 7 December 2007; published 11 March 2008.

[1] The main uncertainty in anthropogenic forcing of the Earth's climate stems from pollution aerosols, particularly their "indirect effect" whereby aerosols modify cloud properties. We develop a new methodology to derive a measurement-based estimate using almost exclusively information from an Earth radiation budget instrument (CERES) and a radiometer (MODIS). We derive a statistical relationship between planetary albedo and cloud properties, and, further, between the cloud properties and column aerosol concentration. Combining these relationships with a data set of satellite-derived anthropogenic aerosol fraction, we estimate an anthropogenic radiative forcing of -0.9 ± 0.4 Wm^{-2} for the aerosol direct effect and of -0.2 ± 0.1 Wm^{-2} for the cloud albedo effect. Because of uncertainties in both satellite data and the method, the uncertainty of this result is likely larger than the values given here which correspond only to the quantifiable error estimates. The results nevertheless indicate that current global climate models may overestimate the cloud albedo effect.

Citation: Quaas, J., O. Boucher, N. Bellouin, and S. Kinne (2008), Satellite-based estimate of the direct and indirect aerosol climate forcing, *J. Geophys. Res.*, *113*, D05204, doi:10.1029/2007JD008962.

1. Introduction

[2] Anthropogenic aerosols exert a "direct effect" by scattering and absorbing sunlight, and "indirect effects" by serving as cloud condensation nuclei, therefore increasing the cloud droplet number concentration and thus cloud albedo ["first aerosol indirect effect" or "cloud albedo effect"; *Twomey*, 1974], as well as cloud cover and cloud liquid water path ["second aerosol indirect effect" or "cloud lifetime effect"; *Albrecht*, 1989]. These aerosol effects lead to an increase in the planetary albedo, thus contributing a negative climate forcing and cooling the Earth system. Aerosol indirect effects have not yet been quantified to satisfaction–an uncertainty that hampers our efforts to predict climate sensitivity and future climate change [*Forster et al.*, 2007; *Andreae et al.*, 2005]. Many estimates of aerosol radiative forcings have been published from modeling studies [*Lohmann and Feichter*, 2005]. Yet, there is no global, observation-based estimate of the combined direct and indirect aerosol forcing. Published estimates of the anthropogenic direct radiative forcing using satellite observations address the total (natural plus anthropogenic) aerosol effect [*Christopher and Zhang*, 2004; *Loeb and Manalo-Smith*, 2005; *Yu et al.*, 2006] or involve modeling assumptions to some extent [*Bellouin et al.*, 2005; *Kaufman et al.*, 2005a]. Some studies also address the aerosol indirect forcing but they rely on the combination of satellite retrievals of cloud microphysical parameters and radiative transfer modeling, and for most of them only apply to a particular region [e.g., *Kaufman and Fraser*, 1997; *Krüger and Graßl*, 2002; *Sekiguchi et al.*, 2003; *Matsui and Pielke*, 2006]. Aerosol indirect radiative forcing estimates from different general circulation models (GCMs) range from -1.9 to -0.5 Wm^{-2} for the cloud albedo effect [*Lohmann and Feichter*, 2005]. However, recent studies constraining models with the observed climate change record [*Anderson et al.*, 2003a] and with satellite data [*Lohmann and Lesins*, 2002; *Quaas and Boucher*, 2005; *Quaas et al.*, 2006] suggest that the aerosol indirect radiative forcing is weaker than this range indicates.

[3] Satellite data are well suited to study aerosol effects on the large scale [*Kaufman et al.*, 2002]. Recent studies identified statistical relationships between aerosol and cloud properties. Aerosol column concentrations have been found to be negatively correlated with cloud top droplet effective radius [CDR; *Nakajima et al.*, 2001; *Bréon et al.*, 2002; *Sekiguchi et al.*, 2003; *Quaas et al.*, 2004; *Kaufman et al.*, 2005b] and positively correlated with cloud droplet number concentration [CDNC; *Nakajima et al.*, 2001; *Sekiguchi et al.*, 2003; *Kaufman et al.*, 2005b; *Quaas et al.*, 2006], cloud liquid water path [LWP; *Sekiguchi et al.*, 2003; *Quaas et al.*, 2004; *Kaufman et al.*, 2005b] and cloud cover [*Loeb and Manalo-Smith*, 2005; *Kaufman et al.*, 2005b; *Kaufman and Koren*, 2006]. These correlations are consistent with our knowledge of the cloud albedo and cloud lifetime effects, respectively. In contrast to previous studies, we investigate here the influence of aerosols on the planetary albedo without the use of a radiative transfer model.

2. Method

[4] We use the broadband short-wave planetary albedo, α, as retrieved by the Clouds and the Earth's Radiant

[1]Max Planck Institute for Meteorology, Hamburg, Germany.
[2]Met Office Hadley Centre, Exeter, UK.

0148-0227/08/2007JD008962$09.00

Energy System [CERES; *Wielicki et al.*, 1996; *Loeb*, 2004; *Loeb et al.*, 2005, 2007], in combination with cloud properties [*Minnis et al.*, 2003] and aerosol optical depth (AOD) as retrieved by the MODerate Resolution Imaging Spectroradiometer [MODIS; *Remer et al.*, 2005]. Both instruments are onboard NASA's Terra platform. The AOD at 0.55 μm comes at $1^\circ \times 1^\circ$ resolution from the MOD08_D3 collection4 data set, corrected for identified biases [*Remer et al.*, 2005] as in the work of *Bellouin et al.* [2005]. CERES albedo, which relies on the flight model 1 applying the User Applied Revisions Rev1, and MODIS retrievals of cloud cover, cloud thermodynamic phase, cloud liquid water path (LWP), cloud optical depth (COD), and cloud top droplet effective radius (CDR) are from the Single Scanner Footprint (SSF) Edition 2B data set at approximately 20 km resolution. Daily data, taken at roughly 10.30 a.m. local time, cover the March 2000–February 2005 period.

[5] COD (τ_c) is a function of CDR (r_e) and LWP (L), and may be written as:

$$\tau_c = \frac{3}{2}\frac{L}{\rho_w r_e} \tag{1}$$

with the density of liquid water, ρ_w. CDNC can be computed from COD and CDR for liquid water clouds assuming adiabaticity [*Brenguier et al.*, 2000; *Schüller et al.*, 2005]:

$$N_d = \gamma \tau_c^{\frac{1}{2}} r_e^{-\frac{5}{2}} \tag{2}$$

with $\gamma = 1.37 \cdot 10^{-5}\mathrm{m}^{-0.5}$ [*Quaas et al.*, 2006]. With this, COD is a function of LWP and CDNC (N_d):

$$\tau_c = \gamma' L^{\frac{5}{6}} N_d^{\frac{1}{3}} \tag{3}$$

where $\gamma' = \gamma^{-\frac{1}{3}} (\frac{2}{5})^{\frac{5}{6}}$.

[6] The albedo of the Earth depends on the albedo of its surface, atmospheric transmittance and reflectance in cloud-free sky (a function of the aerosol optical depth, AOD), cloud cover, and cloud properties. The planetary albedo, α, of a given scene may be described by contributions from the cloudy and clear parts of the scene, where the cloudy part may be further divided into a liquid and ice cloud part:

$$\begin{aligned}\alpha &= (1-f)\alpha^{clr} + f\alpha^{cld} \\ &= (1-f)\alpha^{clr} + f_{liq}\alpha^{liqcld} + f_{ice}\alpha^{icecld}\end{aligned} \tag{4}$$

with f the cloud fraction, f_{liq} and f_{ice} the fraction of all clouds composed of liquid water and ice, respectively ($f_{liq} + f_{ice} = f$), and α^{clr}, α^{cld}, α^{liqcld}, and α^{icecld}, the planetary albedo in the clear part of the scene, and the parts covered by all, liquid and ice clouds, respectively.

[7] In order to evaluate the sensitivity of the planetary albedo to aerosols using satellite data, we fit an empirical expression for the planetary albedo in terms of the aerosol and cloud properties. We adopt the approach of *Loeb* [2004] who showed that the albedo of a cloud scene involving liquid water clouds can be very well described by a sigmoidal fit. This approach is extended here to include also the clear part of the scene, where the planetary albedo also depends on the aerosol optical depth, τ_a, and written in a slightly different notation as:

$$\begin{aligned}\alpha \approx\ & (1-f)[a_1 + a_2 \ln \tau_a] \\ & + f_{liq}[a_3 + a_4(f\tau_c)^{a_5}]^{a_6} + f_{ice}\alpha^{icecld}\end{aligned} \tag{5}$$

where $a_1 - a_6$ are fitting parameters obtained by a multilinear regression. The two terms on the right hand side of this expression describe the planetary albedo in the clear and cloudy parts of the scene, respectively. The contribution of ice clouds to the planetary albedo ($f_{ice}\alpha^{icecld}$) is added here only for completeness. Since in this study, we are interested only in the effect of aerosols on liquid water clouds, the fit is computed by choosing all such situations where only liquid water clouds are present ($f = f_{liq}$).

[8] A prerequisite to estimating the influence of aerosols on planetary albedo via indirect effects is to assess further the influence of aerosol concentration on cloud properties. For this purpose, we compute relationships between cloud properties and AOD as $d\ln f/d\ln\tau_a$, $d\ln L/d\ln\tau_a$, and $d\ln N_d/d\ln\tau_a$ to describe the relative changes of cloud fraction, LWP, and CDNC, respectively, with aerosols. Similar to previous studies [e.g., *Feingold et al.*, 2003; *Quaas and Boucher*, 2005], these relationships are obtained from linear regressions of the respective quantities.

[9] Both the sigmoidal fit for the planetary albedo (equation (5)) and the regressions between cloud quantities and AOD are computed separately for fourteen different regions, notably separating the different oceanic and continental regions (see Figure 1 and Table 1) and for four seasons. The statistics are computed for a subset of the data. Bright surfaces (where the CERES SSF surface classification indicates desert, snow, or ice surfaces) and high latitudes (polewards of 60°), where satellite retrievals may not be reliable, are excluded for the purpose of computing the relationships. For cloudy cases, only liquid water clouds (according to the cloud phase product) are taken. Thin clouds (where LWP < 20 gm^{-2}) are also excluded since neither a clear distinction between aerosols and clouds, nor an accurate retrieval of cloud properties is reliably possible in such cases. Finally, multilayered clouds are excluded since the cloud property retrievals would be ambiguous in such cases. Planetary albedo and cloud properties are used at the original SSF resolution of about 20×20 km^2. For the AOD, data at the resolution of $1^\circ \times 1^\circ$ (latitude $\times$ longitude) is projected to the higher resolution of the SSF product. The reason to use AOD from a coarser-resolved data set is that at such a horizontal resolution, there are usually sufficient temporally coincident retrievals of aerosol concentration and planetary albedo even for cloudy conditions, while aerosol distributions can typically be considered homogeneous [*Anderson et al.*, 2003b]. Aerosol retrievals in the cloud-free part of a $1^\circ \times 1^\circ$ grid-box are assumed to be on average representative for the aerosol concentration at the bases of neighboring clouds.

[10] Figure 2 shows the comparison between the albedo retrieved by CERES and the one computed using the sigmoidal fit for the Northern hemisphere summer over the North Atlantic Ocean. In a vast majority of cases, observed and fitted albedo agree very well. Very small and very large albedos, however, are over- and underestimated by a sig-

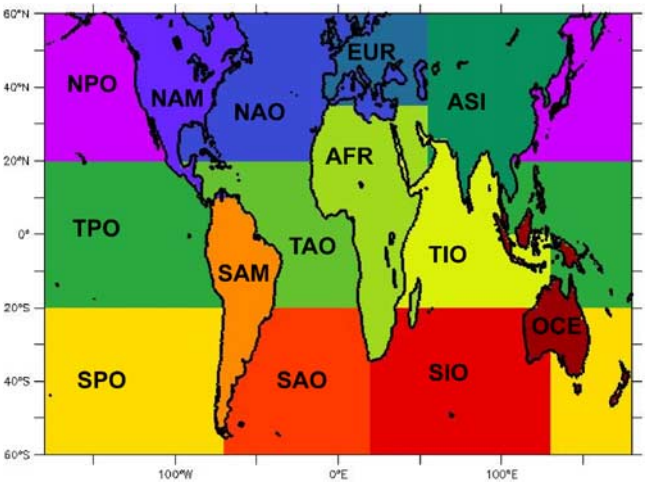

Figure 1. Choice of the fourteen different regions.

moidal fit, respectively. This is due to the fact that the entire variability within a region for a given season cannot be captured entirely by the fit. The particular case shown in Figure 2 is chosen as an example only. The findings described above hold for all other regions and seasons as well.

[11] In Figure 3, the slopes of the regressions of CDNC versus AOD are shown. As expected, they are in all cases - but four - positive at a statistically significant level (according to a Student t-test, $\alpha = 0.01$). The four situations, where the correlation is slightly negative, are for continental regions of the Southern hemisphere and associated with larger relative uncertainties. Over oceans the slopes are larger and the uncertainty on the regression is lower than over land.

3. Radiative Forcing Estimates

[12] The combination of the analytical expression for the planetary albedo (equation (5)) and the regression between cloud properties and AOD allows to compute the influence of aerosols on the planetary albedo:

$$\frac{d\alpha}{d\ln\tau_a} = (1-f)a_2 + (\alpha - (a_1 + a_2\ln\tau_a))\frac{d\ln f}{d\ln\tau_a} + f_{liq}\cdot A(f,\tau_c)\cdot\left[\frac{d\ln f}{d\ln\tau_a} + \frac{5}{6}\frac{d\ln L}{d\ln\tau_a} + \frac{1}{3}\frac{d\ln N_d}{d\ln\tau_a}\right] \quad (6)$$

where the COD has been expanded in its contributions by LWP and CDNC following equation (2). We analyze here only the aerosol effects on liquid water clouds and neglect effects on ice clouds. The latter ones are indeed believed to be small compared to the effects on liquid water clouds [*Lohmann et al.*, 2007]. A detailed description of the derivation of equation (6) and $A(f, \tau_c)$ are given in the Appendix.

[13] The terms of this expression can be evaluated using the fitting parameters $a_1 - a_6$ derived from equation (5) for each region and season, f, f_{liq}, and τ_c from the CERES SSF data set, τ_a from the AOD product, and $d\ln f/d\ln\tau_a$, $d\ln L/d\ln\tau_a$, and $d\ln N_d/d\ln\tau_a$ from the satellite-derived regressions for each region and season. It is important to note that unlike for the calculations of the relationships, we now consider all the situations for the radiative forcing calculations, including those involving bright surfaces, thin clouds, two-layered, or mixed-phase clouds.

[14] The short-wave radiative forcing due to anthropogenic aerosols can then be expressed as

$$\Delta F = \Delta\alpha\cdot\bar{F}^{\downarrow} \quad (7)$$

Table 1. Abbreviations for the Regions and Seasons

DJF	Dec–Jan–Feb
MAM	Mar–Apr–May
JJA	Jun–Jul–Aug
SON	Sep–Oct–Nov
NPO	North Pacific Ocean
NAM	North America
NAO	North Atlantic Ocean
EUR	Europe
ASI	Asia
TPO	Tropical Pacific Ocean
TAO	Tropical Atlantic Ocean
AFR	Africa
TIO	Tropical Indian Ocean
SPO	South Pacific Ocean
SAM	South America
SAO	South Atlantic Ocean
SIO	South Indian Ocean
OCE	Oceania

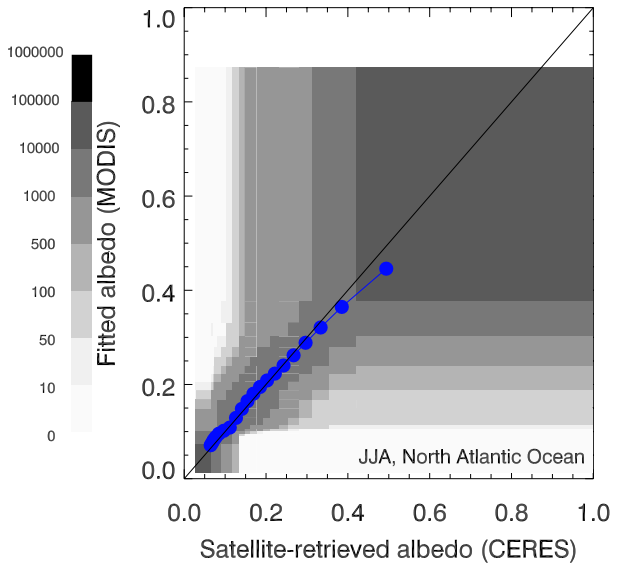

Figure 2. Joint histogram of albedo directly retrieved from the CERES instrument and the one fitted from aerosol and cloud properties retrieved from MODIS. Shown here is the example for the North Atlantic region, Northern hemisphere summer (JJA)-results for the other regions and seasons are similar. The width of the 20 bins along the x- and y-axes are chosen so that the sum of data points along the other axis is constant. The gray scale shows the number of points within each box. The blue line shows the mean modeled albedo in each bin of satellite-derived albedo.

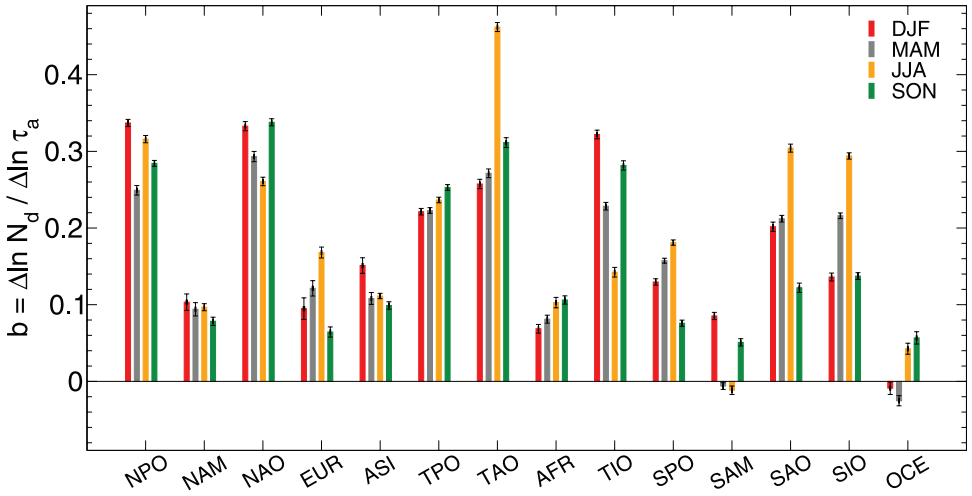

Figure 3. Slopes of the linear regression ln CDNC versus ln AOD for the different regions and seasons. Error bars show 10 times the standard deviation (a list of abbreviations is given in Table 1).

where $\bar{F}^{\downarrow}$ denotes the daily mean incoming solar radiation, and the change in planetary albedo due to anthropogenic aerosols, $\Delta\alpha$, can be computed as

$$\Delta\alpha = \frac{d\alpha}{d\ln\tau_a}\left[\ln\tau_a - \ln\left(\tau_a - \tau_a^{ant}\right)\right] \tag{8}$$

[15] In equation (8), $\frac{d\alpha}{d\ln\tau_a}$ is obtained from equation (6), τ_a from the satellite data, and the anthropogenic AOD, τ_a^{ant}, from the data set derived by *Bellouin et al.* [2005]. The distribution of the anthropogenic AOD is shown in Figure 4. It is derived from a combination of satellite-derived aerosol fine-mode fraction, aerosol absorption index, and surface wind speed over oceans on a daily basis (in order to distinguish fossil fuel- and biomass burning pollution from sea salt and dust aerosols), and from model-estimated anthropogenic fractions over land using the AEROCOM global aerosol model ensemble. We acknowledge that future improvements of this product are necessary in particular over continental areas.

[16] Pasting equation (6) into equation (8), we can now distinguish the different contributions to the anthropogenic aerosol forcing. While the aerosol forcings on clouds can be regarded at first order independent on the solar zenith angle [*Boucher*, 1995], this is not the case for the aerosol direct forcing. For the latter we therefore estimate the instantaneous forcing at the satellite overpass time, and apply a scaling factor, r_F, which is the ratio of the daily mean to instantaneous forcings as computed with a radiative transfer model by *Bellouin et al.* [2005]. The direct forcing is thus

$$\Delta F^{ADE} = (1-f)a_2\left[\ln\tau_a - \ln\left(\tau_a - \tau_a^{ant}\right)\right]F^{\downarrow}r_F \tag{9}$$

with the incident solar flux at the time of the satellite overpass, $F^{\downarrow}$. The forcing by the cloud albedo effect is

$$\Delta F^{AIE} = f_{liq}\cdot A(f,\tau_c)\frac{1}{3}\cdot\frac{d\ln N_d}{d\ln\tau_a}\left[\ln\tau_a - \ln\left(\tau_a - \tau_a^{ant}\right)\right]\bar{F}^{\downarrow} \tag{10}$$

and the remainder,

$$\Delta F^{AIE2} = \left[\left(\alpha - (a_1 + a_2\ln\tau_a)\right)\frac{d\ln f}{d\ln\tau_a} + f_{liq}\cdot A(f,\tau_c)\cdot\left(\frac{d\ln f}{d\ln\tau_a} + \frac{5}{6}\frac{d\ln L}{d\ln\tau_a}\right)\right]\cdot\left[\ln\tau_a - \ln\left(\tau_a - \tau_a^{ant}\right)\right]\bar{F}^{\downarrow} \tag{11}$$

may correspond to the cloud lifetime effect, but other processes or artifacts may play a role as well. The term includes a contribution from the increase in cloud cover and a second one from the increase in LWP with increasing aerosol concentrations.

[17] Figure 5 shows the spatial distribution of the radiative forcings for the five-year average radiative forcing by the direct and cloud albedo aerosol effects as defined above. On a global (60°S to 60°N) average, the direct forcing is -0.9 Wm^{-2}, and the cloud albedo effect, -0.2 Wm^{-2}. The direct forcing is stronger over land (-1.8 Wm^{-2}) than over ocean (-0.7 Wm^{-2}). In contrast, the cloud albedo aerosol effect is generally stronger over oceans (-0.2 Wm^{-2} versus -0.1 Wm^{-2}) even though anthropogenic aerosol sources are on land. This is because maritime clouds are more susceptible to changes in aerosol concentrations as shown in Figure 3. The forcing is particularly strong over the extended stratus/stratocumulus decks off the west coasts of Southern Africa and South America, and downwind of pollution originating in Asia. Both effects are stronger in the Northern than in the Southern hemisphere (-1.3 Wm^{-2} versus -0.4 Wm^{-2} for the direct, and -0.3 Wm^{-2} vversus -0.1 Wm^{-2} for the cloud albedo effect), where anthropogenic aerosol sources are weaker.

4. Discussion

[18] From comparisons with surface measurements, the uncertainty in MODIS-retrieved COD has been quantified as 21% [*Minnis et al.*, 2004]. Since cloud fraction is retrieved at sub-pixel scale (250 m resolution), the error at the much larger SSF scale is assumed negligible (assuming

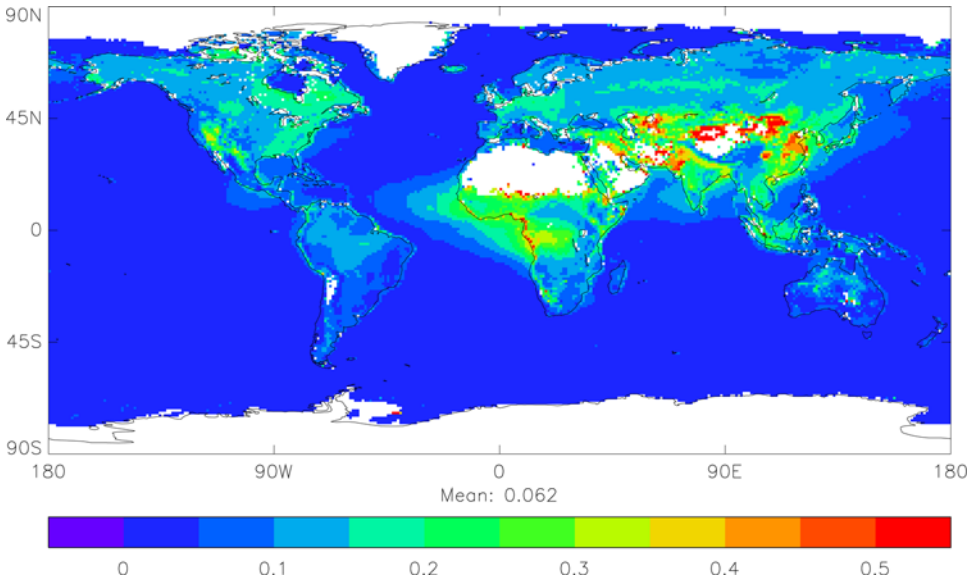

Figure 4. Five-year (March 2000–February 2005) averaged anthropogenic AOD derived from satellite data as in the work of *Bellouin et al.* [2005].

statistical errors), as is the determination of the cloud thermodynamic phase. From satellite intercomparisons, the uncertainty in radiative flux retrievals by CERES is estimated as 5% [*Loeb*, 2004]. The uncertainty in AOD is 5% over ocean and 10% over land according to the study by *Remer et al.* [2005]; and the uncertainty in the anthropogenic AOD as well as in the conversion factor r_F is given as 15% by *Bellouin et al.* [2005]. Uncertainties in the statistical relationships and fitting parameters are given as 1σ standard deviations. The propagation of error computation yields the influence of these relative uncertainties in the input quantities on the computed radiative forcings, ± 0.4 Wm^{-2} for the direct, and ± 0.1 Wm^{-2} for the cloud albedo effects. It should be noted that we refer here to the published quantifiable uncertainties in the satellite retrievals. Limitations of our method (e.g., the need to select not-too-thin single-layer clouds to compute the statistical relationships) or in satellite data (e.g., the overestimation of AOD over land [*Levy et al.*, 2007]) contribute to the overall uncertainty but cannot be quantified. It seems thus likely that the given uncertainty range does not give absolute bounds on the direct and indirect aerosol radiative forcings.

[19] Satellite retrievals of AOD can be biased high in the vicinity of clouds due to the higher relative humidity [*Haywood et al.*, 1997; *Koren et al.*, 2007], and can also be artificially increased due to scattering of solar radiation from the sides of neighboring cloud ["3D effect"; *Wen et al.*, 2007]. Since both biases may be particularly high for thick clouds, the correlation between CDNC (computed from COD) and AOD might thus be still too steep, so that our estimate of the first aerosol indirect effect could be still be overestimated. However, since we use AOD averaged over a relatively large domain, and since consistent AOD is used for the statistical computations and for the anthropogenic AOD in the radiative forcing estimates, these biases should not impact very much the radiative forcing estimates for the direct and first indirect aerosol effects. To clearly determine the uncertainty inferred by the satellite retrieval method, however, our study will have to be re-done with future improved satellite products. The exclusion of cases where the satellite data are not reliable for the computations of the statistical relationships also introduces an uncertainty. However, for the computation of the forcing on the basis of these relationships, all different scenes are taken into account assuming the relationships computed for the more reliable scenes are also valid for thin and two-layered clouds. Meteorological conditions affect both aerosol concentrations and clouds. However, our method separates the contribution of changes in CDNC, LWP, and cloud cover to the changes in planetary albedo. Thus meteorological conditions are to some extent constrained for the computation of the first aerosol indirect effect (the change of cloud albedo through changes in CDNC). This argument, however, does not hold for the relationship between AOD and cloud fraction.

[20] As for the cloud lifetime effect, the positive correlations between cloud fraction and AOD, and between LWP and AOD (Figure 6), in combination with the fitted expression for planetary albedo, translate into radiative effects of -3.1 Wm^{-2} and -0.1 Wm^{-2}, respectively. It must be noted that in particular the interpretation of the often-found positive relationship between cloud fraction and AOD as a representation of the cloud lifetime aerosol effect is largely debated [*Kaufman et al.*, 2005c; *Loeb and Manalo-Smith*, 2005; *Zhang et al.*, 2005; *Lohmann et al.*, 2006]. It is not clear how much of this radiative effect is due to aerosol effects on cloud, and how much is due to cloud and humidity effects on aerosols. The impossibility to uniquely distinguish cloudy and clear skies [*Haywood et al.*, 1997; *Charlson et al.*, 2007; *Koren et al.*, 2007] and inaccuracies in the satellite retrievals neglecting "3D" cloud effects on radiation [*Wen et al.*, 2007] may play important roles as well. We thus refrain here from interpreting the correlation between AOD and cloud fraction as an aerosol indirect

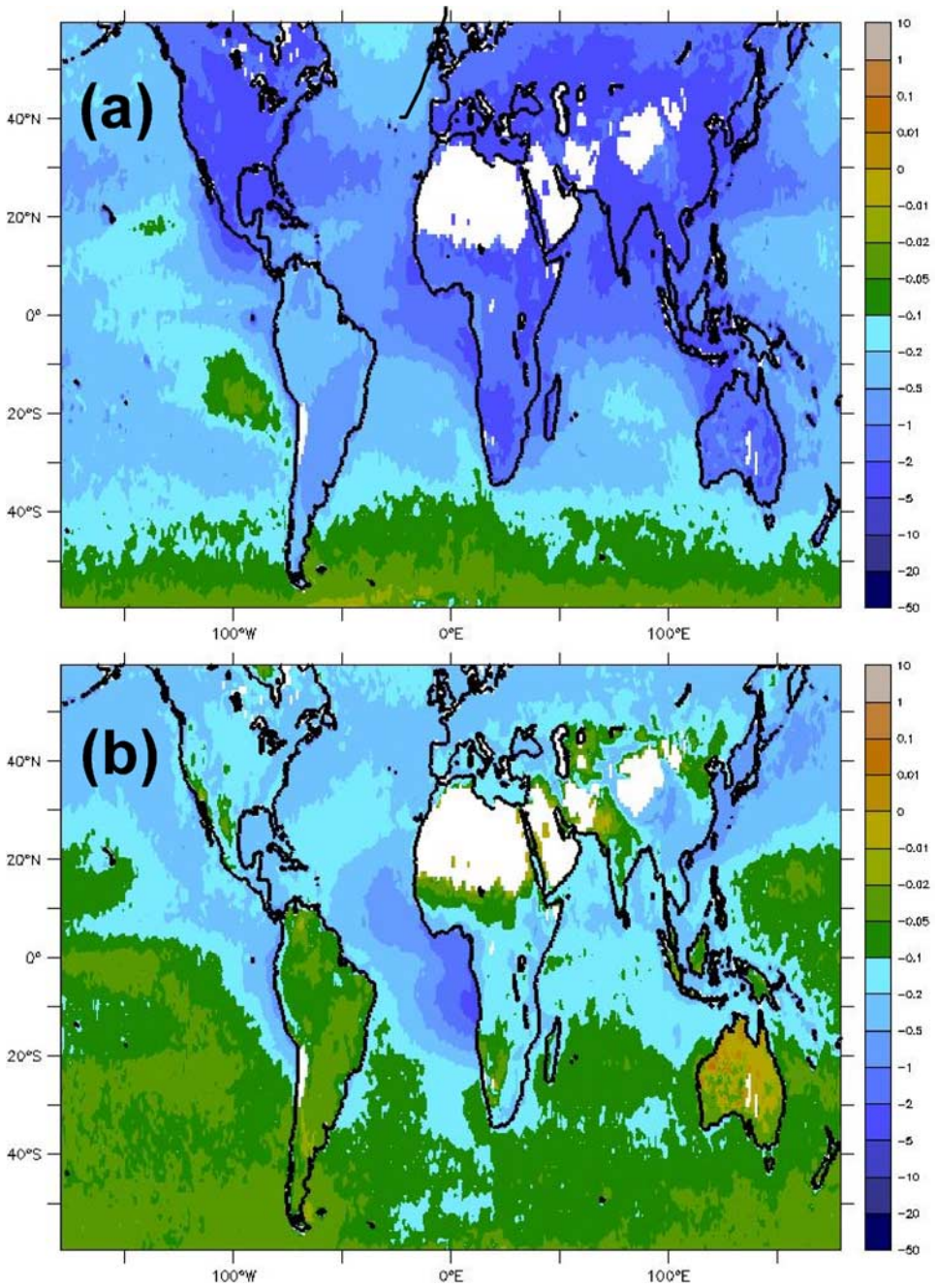

Figure 5. Five-year (March 2000–February 2005) averaged radiative forcing by (a) the direct and (b) cloud albedo aerosol effects [Wm^{-2}].

effect. In climate models, the cloud lifetime effect results in an increase in LWP, but in a very small perturbation of the cloud cover [*Feichter et al.*, 2004; *Lohmann et al.*, 2006]. This might indicate that much of the correlation between cloud fraction and AOD is not due to the cloud lifetime effect (but rather some or all of the other effects mentioned), whereas the correlation between LWP and AOD might reflect an aerosol effect. This would be consistent with the finding by climate models that the cloud albedo and cloud lifetime effects are roughly of the same order of magnitude [*Lohmann and Feichter*, 2005]. For a conclusion on the cloud lifetime effect, however, further research is necessary.

5. Conclusions

[21] The aerosol direct forcing derived here is consistent with other measurement-based estimates [*Bellouin et al.*, 2005; *Kaufman et al.*, 2005a], but larger than most model-based estimates. This discrepancy may be partly due to the fact that satellite retrievals of aerosols are not available over bright surfaces such as deserts, snow- or ice-covered surfaces, or low-level clouds, where the direct forcing may even

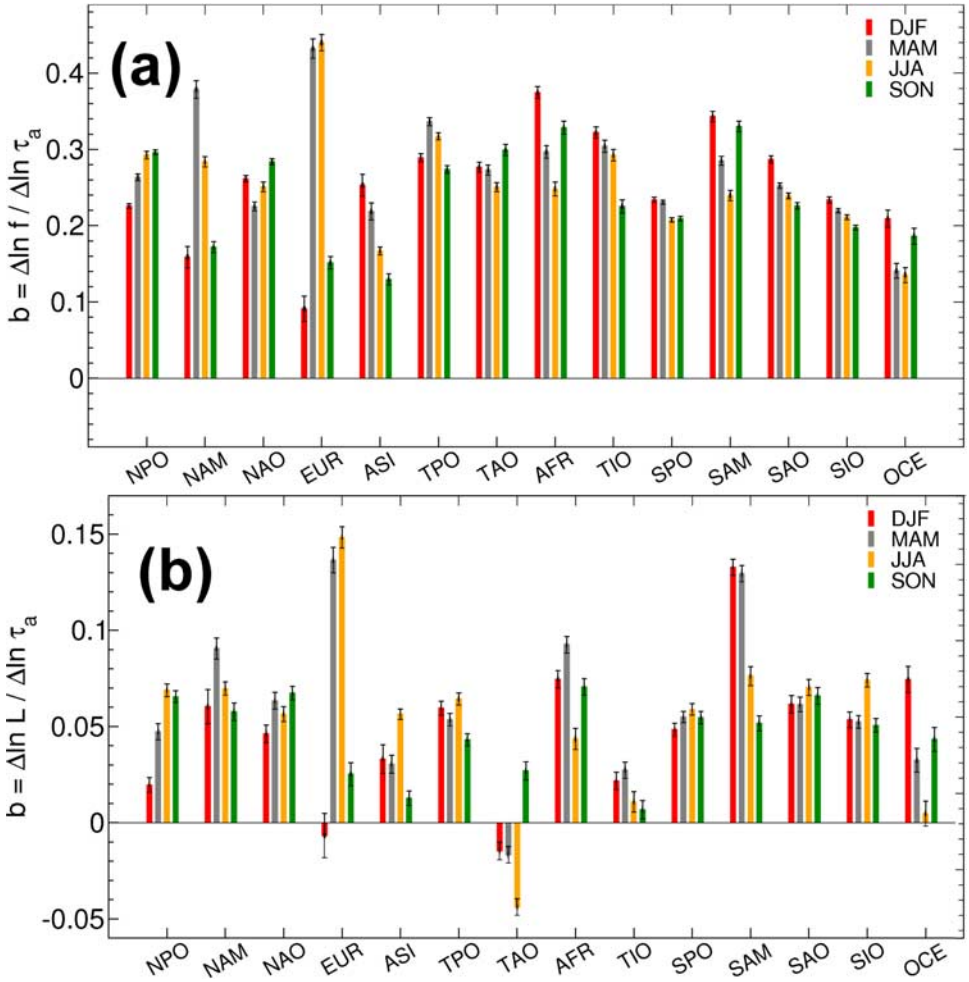

Figure 6. As Figure 3, but for the linear regressions (a) ln f versus ln AOD and (b) ln L versus ln AOD.

become positive. Sensitivity studies with a radiative transfer model [S. Kinne, Aerosol direct radiative forcing with an Aeronet touch, *Atmos. Res.*] indicate that these effects might add up to a reduction of the forcing by up to 30–60%. The forcing by the cloud albedo aerosol effect is much smaller than most model-based estimates [*Lohmann and Feichter*, 2005] but consistent with estimates from models constrained by satellite observations [*Lohmann and Lesins*, 2002; *Quaas et al.*, 2006]. It is consistent, too, with the value found by *Sekiguchi et al.* [2003] from a combination of statistical relationships between cloud properties and aerosol concentration from POLDER satellite data and radiative transfer calculations (they estimate -0.2 Wm^{-2} with much larger values over ocean than over land). The overall aerosol effect we find here is also consistent with estimates from the observed climate change record [*Anderson et al.*, 2003a], though with a magnitude in the upper range given by such studies, pointing to a relatively strong sensitivity of the climate system [*Andreae et al.*, 2005]. Future studies using the upcoming data set retrieved from spaceborne active remote sensing instruments (radar, lidar) will test the assumptions made in this study concerning the representativeness of aerosol column for aerosol indirect effect calculations and the contributions of bright surface regions to the aerosol radiative forcing. Also, potential aerosol effects on ice clouds may be considered in future studies.

Appendix A

[22] We take the derivative of equation (5) with respect to $\ln\tau_a$:

$$\frac{d\alpha}{d\ln\tau_a} = \frac{d}{d\ln\tau_a}[(1-f)[a_1 + a_2\ln\tau_a] + \frac{d}{d\ln\tau_a}\left[f_{liq}[a_3 + a_4(f\tau_c)^{a_5}]^{a_6}\right] + \frac{d}{d\ln\tau_a}\left[f_{ice}\alpha^{icecld}\right] \quad \text{(A1)}$$

[23] Since we are interested here only in the influence of aerosols on liquid clouds, we neglect aerosol effects on ice clouds here assuming the last term on the right hand side to be zero. Then,

$$\frac{d\alpha}{d\ln\tau_a} = (1-f)a_2 - [a_1 + a_2\ln\tau_a]\frac{df}{d\ln\tau_a} + \left[[a_3 + a_4(f\tau_c)^{a_5}]^{a_6}\frac{df_{liq}}{d\ln\tau_a}\right.$$

$$+ f_{liq} a_6 [a_3 + a_4 (f\tau_c)^{a_5}]^{a_6 - 1} a_4 a_5 (f\tau_c)^{a_5 - 1} \cdot \left(f \frac{d\tau_c}{d \ln \tau_a} + \tau_c \frac{df}{d \ln \tau_a} \right) \Bigg] \quad \text{(A2)}$$

which can be rewritten as

$$\begin{aligned} \frac{d\alpha}{d \ln \tau_a} &= (1 - f) a_2 \\ &+ \Bigg[- [a_1 + a_2 \ln \tau_a] \frac{df}{d \ln \tau_a} \\ &+ [a_3 + a_4 (f\tau_c)^{a_5}]^{a_6} \frac{df_{liq}}{d \ln \tau_a} \Bigg] \\ &+ f_{liq} a_6 [a_3 + a_4 (f\tau_c)^{a_5}]^{a_6 - 1} a_4 a_5 (f\tau_c)^{a_5 - 1} \\ &\cdot \left(f \frac{d\tau_c}{d \ln \tau_a} + \tau_c \frac{df}{d \ln \tau_a} \right) \\ &= [1] + [2] + [3] \end{aligned} \quad \text{(A3)}$$

[24] Since $\frac{df}{d \ln \tau_a} = f \frac{d \ln f}{d \ln \tau_a}$ and $\frac{df_{liq}}{d \ln \tau_a} = f_{liq} \frac{d \ln f_{liq}}{d \ln \tau_a}$, the second term can be further rewritten as

$$\begin{aligned} [2] = & - f [a_1 + a_2 \ln \tau_a] \frac{d \ln f}{d \ln \tau_a} \\ & + f_{liq} [a_3 + a_4 (f\tau_c)^{a_5}]^{a_6} \frac{d \ln f_{liq}}{d \ln \tau_a} \end{aligned} \quad \text{(A4)}$$

[25] Since we analyze only the influence of aerosols on liquid water clouds, here $\frac{d \ln f_{liq}}{d \ln \tau_a} = \frac{d \ln f}{d \ln \tau_a}$. The second term is then

$$\begin{aligned} [2] &= \left[f_{liq} [a_3 + a_4 (f\tau_c)^{a_5}]^{a_6} - f [a_1 + a_2 \ln \tau_a] \right] \frac{d \ln f}{d \ln \tau_a} \\ &= \left[(1 - f)(a_1 + a_2 \ln \tau_a) + f_{liq} [a_3 + a_4 (f\tau_c)^{a_5}]^{a_6} \right. \\ &\quad \left. - (a_1 + a_2 \ln \tau_a) \right] \frac{d \ln f}{d \ln \tau_a} \\ &= [\alpha - (a_1 + a_2 \ln \tau_a)] \frac{d \ln f}{d \ln \tau_a} \end{aligned} \quad \text{(A5)}$$

[26] Introducing similar logarithmic derivatives, $\frac{d \ln \tau_c}{d \ln \tau_a}$ and $\frac{d \ln f}{d \ln \tau_a}$, and further use of equation (3), the third term can be rewritten as

$$\begin{aligned} [3] &= f_{liq} f a_4 a_5 a_6 [a_3 + a_4 (f\tau_c)^{a_5}]^{a_6 - 1} (f\tau_c)^{a_5} \\ &\quad \cdot \left(\frac{d \ln \tau_c}{d \ln \tau_a} + \frac{d \ln f}{d \ln \tau_a} \right) \\ &= f_{liq} f a_4 a_5 a_6 [a_3 + a_4 (f\tau_c)^{a_5}]^{a_6 - 1} (f\tau_c)^{a_5} \\ &\quad \cdot \left(\frac{d \ln f}{d \ln \tau_a} + \frac{5}{6} \frac{d \ln L}{d \ln \tau_a} + \frac{1}{3} \frac{d \ln N_d}{d \ln \tau_a} \right) \\ &= f_{liq} \cdot A(f, \tau_c) \cdot \left(\frac{d \ln f}{d \ln \tau_a} + \frac{5}{6} \frac{d \ln L}{d \ln \tau_a} + \frac{1}{3} \frac{d \ln N_d}{d \ln \tau_a} \right) \end{aligned} \quad \text{(A6)}$$

where $A(f, \tau_c) = a_4 a_5 a_6 [a_3 + a_4 (f\tau_c)^{a5}]^{a6-1} (f\tau_c)^{a5}$.

[27] **Acknowledgments.** CERES SSF data were obtained from the NASA Langley Research Center Atmospheric Sciences Data Center. MODIS data used in this study were acquired as part of NASA(tm)s Earth Science Enterprise. The MODIS Science Teams developed the algorithms for the AOD retrievals. The data were processed by the MODIS Adaptive Processing System and the Goddard Distributed Active Archive (DAAC) and are archived and distributed by the Goddard DAAC. The authors would like to thank the data distribution centers for their support, and Norman Loeb, Sundar Christopher, and Johann Feichter for helpful discussions. JQ was supported by an Emmy Noether grant of the German Research Foundation (DFG) and acknowledges the hospitality of the Met Office Hadley Centre. The work of OB and NB forms part of the Integrated Climate Programme of the UK Department for Environment, Food and Rural Affairs (Defra) and Ministry of Defence.

References

Albrecht, B. (1989), Aerosols, cloud microphysics, and fractional cloudiness, *Science*, *245*, 1227–1230.

Anderson, T. L., R. J. Charlson, S. E. Schwartz, R. Knutti, O. Boucher, H. Rodhe, and J. Heintzenberg (2003a), Climate forcing by aerosols-A hazy picture, *Science*, *300*, 1103–1104.

Anderson, T. L., R. J. Charlson, D. M. Winker, J. A. Ogren, and K. Holmén (2003b), Mesoscale variations of tropospheric aerosols, *J. Atmos. Sci.*, *60*, 119–136.

Andreae, M. O., C. D. Jones, and P. M. Cox (2005), Strong present-day aerosol cooling implies a hot future, *Nature*, *435*, doi:10.1038/nature.03671.

Bellouin, N., O. Boucher, J. Haywood, and M. S. Reddy (2005), Global estimate of aerosol direct radiative forcing from satellite measurements, *Nature*, *438*, 1138–1141.

Boucher, O. (1995), Étude de quelques interactions aérosol-nuage-rayonnement: Modélisation et simulations avec un modèle de circulation générale, Ph.D. thesis, Université P. et M. Curie.

Brenguier, J. L., H. Pawlowska, L. Schüller, R. Preusker, J. Fischer, and Y. Fouquart (2000), Radiative properties of boundary layer clouds: Droplet effective radius versus number concentration, *J. Atmos. Sci.*, *57*, 803–821.

Bréon, F.-M., D. Tanré, and S. Generoso (2002), Aerosol effect on cloud droplet size monitored from satellite, *Science*, *295*, 834–838.

Charlson, R. J., A. S. Ackerman, F. A.-M. Bender, T. L. Anderson, and Z. Liu (2007), On the climate forcing consequences of the albedo continuum between cloudy and clear air, *Tellus*, *59*(4), 715–727.

Christopher, S. A., and J. Zhang (2004), Cloud-free shortwave aerosol radiative effect over oceans: Strategies for identifying anthropogenic forcing from Terra satellite measurements, *Geophys. Res. Lett.*, *31*, L18101, doi:10.1029/2004GL020510.

Feichter, J., E. Roeckner, U. Lohmann, and B. Liepert (2004), Nonlinear aspects of the climate response to greenhouse gas and aerosol forcing, *J. Clim.*, *17*, 2384–2398.

Feingold, G., W. L. Eberhard, D. E. Veron, and M. Previdi (2003), First measurements of the Twomey indirect effect using ground-based remote sensors, *Geophys. Res. Lett.*, *30*(1287), 1287, doi:10.1029/2002GL016633.

Forster, P., V. Ramaswamy, P. Artaxo, T. Berntsen, R. Betts, D. Fahey, J. Haywood, J. Lean, D. Lowe, G. Myhre, J. Nganga, R. Prinn, G. Raga, M. Schulz, and R. Van Dorland (2007), *Climate Change 2007: The Physical Science Basis. Contribution of Working Group I to the Fourth Assessment Report of the Intergovernmental Panel on Climate Change*, chap. Changes in Atmospheric Constituents and in Radiative Forcing, pp. 129–243, Cambridge University Press, Cambridge, United Kingdom and New York, NY, USA.

Haywood, J. M., V. Ramaswamy, and L. J. Donner (1997), A limited-area-model case study of the effects of sub-grid scale variations in relative humidity and cloud upon the direct radiative forcing of sulfate aerosol, *Geophys. Res. Lett.*, *24*, 143–146.

Kaufman, Y. J., and R. S. Fraser (1997), The effect of smoke particles on clouds and climate forcing, *Science*, *277*, 1636–1639.

Kaufman, Y. J., and I. Koren (2006), Smoke and pollution aerosol effect on cloud cover, *Science*, *313*, 655–658.

Kaufman, Y. J., D. Tanré, and O. Boucher (2002), A satellite view of aerosols in the climate system, *Nature*, *419*, 215–223.

Kaufman, Y. J., O. Boucher, D. Tanré, M. Chin, L. A. Remer, and T. Takemura (2005a), Aerosol anthropogenic component estimated from satellite data, *Geophys. Res. Lett.*, *32*, L17804, doi:10.1029/2005GL023125.

Kaufman, Y. J., I. Koren, L. A. Remer, D. Rosenfeld, and Y. Rudich (2005b), The effect of smoke, dust, and pollution aerosol on shallow cloud development over the Atlantic Ocean, *Proc. Natl. Acad. Sci.*, *102*, 11,207–11,212.

Kaufman, Y. J., L. A. Remer, D. Tanré, R. R. Li, R. Kleidman, S. Mattoo, R. Levy, T. Eck, B. N. Holben, C. Ichoku, J. Martins, and I. Koren (2005c), A critical examination of the residual cloud contamination and diurnal sampling effects on MODIS estimates of aerosol over ocean, *IEEE Trans. Geosci. Remote Sens.*, *43*, 2886–2897.

Koren, I., L. A. Remer, Y. J. Kaufman, Y. Rudich, and J. V. Martins (2007), On the twilight zone between clouds and aerosols, *Geophys. Res. Lett.*, *34*, (L08805), doi:10.1029/2007GL029253.

Krüger, O., and H. Graßl (2002), The indirect aerosol effect over Europe, *Geophys. Res. Lett.*, *29*(19), 1925–1929, 1925, doi:10.1029/2001GL014081.

Levy, R., L. A. Remer, S. Mattoo, E. F. Vermote, and Y. J. Kaufman (2007), Second-generation operational algorithm: Retrieval of aerosol properties over land from inversion of Moderate Resolution Imaging Spectroradiometer spectral reflectance, *J. Geophys. Res.*, *112*, (D13211), doi:10.1029/2006JD007811.

Loeb, N. (2004), Angular models: Instantaneous and ensemble accuracy, in *1st CERES-II Science Team Meeting Proceedings*, NCAR, Boulder, Colorado.

Loeb, N. G., and N. Manalo-Smith (2005), Top-of-atmosphere direct radiative effect of aerosols over global oceans from merged CERES and MODIS observations, *J. Clim.*, *18*, 3506–3526, doi:10.1175/JCLI3504.1.

Loeb, N. G., S. Kato, K. Loukachine, and N. Manalo-Smith (2005), Angular distribution models for top-of-atmosphere radiative flux estimation from the Clouds and the Earth's Radiant Energy System instrument on the Terra satellite. Part I: Methodology, *J. Atmos. Oceanic Technol.*, *22*, 338–351.

Loeb, N. G., B. A. Wielicki, W. Su, K. Loukachine, W. Sun, T. Wong, K. J. Priestley, G. Matthews, W. F. Miller, and R. Davies (2007), Multi-instrument comparison of top-of-atmosphere reflected solar radiation, *J. Clim.*, *20*, 575–591.

Lohmann, U., and J. Feichter (2005), Global indirect aerosol effects: A review, *Atmos. Chem. Phys.*, *5*, 715–737.

Lohmann, U., and G. Lesins (2002), Stronger constraints on the anthropogenic indirect aerosol effect, *Science*, *298*, 1012–1015.

Lohmann, U., I. Koren, and Y. J. Kaufman (2006), Disentangling the role of microphysical and dynamical effects in determining cloud properties over the Atlantic, *Geophys. Res. Lett.*, *33*, L09802, doi:10.1029/2005GL024625.

Lohmann, U., P. Stier, C. Hoose, S. Ferrachat, S. Kloster, E. Roeckner, and J. Zhang (2007), Cloud microphysics and aerosol indirect effects in the global climate model ECHAM5-HAM, *Atmos. Chem. Phys.*, *7*, 3425–3446.

Matsui, T., and R. A. Pielke Sr. (2006), Measurement-based estimation of the spatial gradient of aerosol radiative forcing, *Geophys. Res. Lett.*, *33*, L11813, doi:10.1029/2006GL025974.

Minnis, P., D. F. Young, S. Sun-Mack, P. W. Heck, D. R. Doelling, and Q. Z. Trepte (2003), CERES cloud property retrievals from imagers on TRMM, Terra, and Aqua, in *Proc. SPIE 10th International Symposium on Remote Sensing: Conference on Remote Sensing of Clouds and the Atmosphere VII*, vol. 5235, pp. 37–48, Barcelona, Spain.

Minnis, P., D. F. Young, S. Sun-Mack, Q. Trepte, D. R. Doelling, D. A. Spangenberg, and P. W. Heck (2004), Ceres cloud products, in *1st CERES-II Science Team Meeting Proceedings*, NCAR, Boulder, Colorado.

Nakajima, T., A. Higurashi, K. Kawamoto, and J. E. Penner (2001), A possible correlation between satellite-derived cloud and aerosol microphysical parameters, *Geophys. Res. Lett.*, *28*, 1171–1174.

Quaas, J., and O. Boucher (2005), Constraining the first aerosol indirect radiative forcing in the LMDZ GCM using POLDER and MODIS satellite data, *Geophys. Res. Lett.*, *32*, L17814, doi:10.1029/2005GL023850.

Quaas, J., O. Boucher, and F.-M. Bréon (2004), Aerosol indirect effects in POLDER satellite data and in the LMDZ GCM, *J. Geophys. Res.*, 109, D08205, doi:10.1029/2003JD004317.

Quaas, J., O. Boucher, and U. Lohmann (2006), Constraining the total aerosol indirect effect in the LMDZ and ECHAM4 GCMs using MODIS satellite data, *Atmos. Chem. Phys.*, *6*, 947–955.

Remer, L. A., Y. J. Kaufman, S. Mattoo, J. V. Martins, C. Ichoku, R. C. Levy, R. G. Kleidman, D. Tanré, D. A. Chu, R. R. Li, T. F. Eck, E. Vermote, and B. N. Holben (2005), The MODIS algorithm, products and validation, *J. Atmos. Sci.*, *62*, 947–973, doi:10.1175/JAS3385.1.

Schüller, L., R. Bennartz, J. Fischer, and J.-L. Brenguier (2005), An algorithm for the retrieval of droplet number concentration and geometrical thickness of stratiform marine boundary layer clouds applied to MODIS radiometric observations, *J. Appl. Meteorol.*, *44*, 28–38.

Sekiguchi, M. T., K. Suzuki, K. Kawamoto, A. Higurashi, D. Rosenfeld, I. Sano, and S. Mukai (2003), A study of the direct and indirect effects of aerosols using global satellite data sets of aerosol and cloud parameters, *J. Geophys. Res.*, *108*(D22), 4699, doi:10.1029/2002JD003359.

Twomey, S. (1974), Pollution and the planetary albedo, *Atmos. Environ.*, *8*, 1251–1258.

Wen, G., A. Marshak, R. F. Cahalan, L. A. Remer, and R. G. Kleidman (2007), 3-D aerosol-cloud radiative interaction observed in collocated MODIS and ASTER images of cumulus cloud fields, *J. Geophys. Res.*, *112*, (D13204), doi:10.1029/2006JD008267.

Wielicki, B. A., B. R. Barkstrom, E. F. Harrison, R. B. L. III, G. L. Smith, and J. E. Cooper (1996), Clouds and the Earth's Radiant Energy System (CERES): An Earth observing system experiment, *Bull. Am. Meteorol. Soc.*, *77*, 853–868.

Yu, H., Y. J. Kaufman, M. Chin, G. Feingold, L. A. Remer, T. L. Anderson, Y. Balkanski, N. Bellouin, O. Boucher, S. Christopher, P. DeCola, R. Kahn, D. Koch, N. Loeb, M. S. Reddy, M. Schulz, T. Takemura, and M. Zhou (2006), A review of measurement-based assessment of aerosol direct radiative effect and forcing, *Atmos. Chem. Phys.*, *6*, 613–666.

Zhang, J., J. S. Reid, and B. N. Holben (2005), An analysis of potential cloud artifacts in MODIS over ocean aerosol optical thickness products, *Geophys. Res. Lett.*, *32*, L15803, doi:10.1029/2005GL023254.

N. Bellouin and O. Boucher, Met Office Hadley Centre, FitzRoy Road, EX1 3PB Exeter, UK.

S. Kinne and J. Quaas, Max Planck Institute for Meteorology, Bundesstraße 53, 20146 Hamburg, Germany. (johannes.quaas@zmaw.de)